Article ID: 1000-324X(2023)10-1223-07 **DOI:** 10.15541/jim20230091

Fabrication and Properties of AlN-SiC Multiphase Ceramics *via* Low Temperature Reactive Melt Infiltration

SUN Xiaofan[1,2], CHEN Xiaowu[1,2], JIN Xihai[1,2], KAN Yanmei[1,2], HU Jianbao[1,2], DONG Shaoming[1,2]

(1. State Key Laboratory of High Performance Ceramics and Superfine Microstructure, Shanghai Institute of Ceramics, Chinese Academy of Sciences, Shanghai 200050, China; 2. Center of Materials Science and Optoelectronics Engineering, University of Chinese Academy of Sciences, Beijing 100049, China)

Abstract: AlN-SiC multiphase ceramics possess robust mechanical strength, high thermal conductivity and good oxidization resistance, and show great potential as the matrix material of fiber reinforced ceramic matrix composites. In this work, AlN-SiC multiphase ceramics were fabricated *via* low temperature reactive melt infiltration of Si-Al alloy into porous C-Si_3N_4 preforms. Influence of Si-Al source on the melt infiltration process was studied, and impact of residual silicon on the mechanical and thermal properties of the AlN-SiC ceramics was investigated. It was found that an Al–O layer was *in-situ* formed at the interface between Si-Al melt and C-Si_3N_4 preform, when Si-Al powder was used as the infiltration medium. This seriously retarded the melt infiltration process and made the penetration of Si-Al melt into the C-Si_3N_4 preform hardly possible. However, when Si-Al ingot was used as the infiltration medium, a well infiltration of Si-Al melt into the C-Si_3N_4 preform occurred, which led to the formation of dense AlN-SiC ceramics. Mechanical and thermal property measurements indicated that the strength of the AlN-SiC ceramics was significantly improved as the residual silicon content in it was reduced, while a reverse trend was observed for the thermal conductivity. AlN-SiC ceramics with 4%(in mass) residual silicon showed a high strength of 320.1 MPa, nearly comparable to that of conventional reaction bonded SiC, although its thermal conductivity was modest (26.3 $W \cdot m^{-1} \cdot K^{-1}$). The fundamental reasons for the above phenomena were discussed. This study is of great significance for the preparation of SiC_f/AlN-SiC composites by low temperature reactive melt infiltration.

Key words: reactive melt infiltration (RMI); AlN-SiC; mechanical property; thermal conductivity

Continuous SiC fiber reinforced SiC ceramic matrix composites (SiC_f/SiC) is regarded as a promising candidate for using as hot-end components of new generation high-performance aero-engine due to its prominent advantages over traditional superalloys, such as low density, high temperature resistance, oxidation resistance, high specific strength and high specific modulus[1-3]. Especially, SiC_f/SiC prepared by reactive melt infiltration (RMI) method is considered even more favorable, because of its low porosity, good thermal conductivity, high environmental endurability and low preparation cost[4-5] in comparison with its counterparts prepared by other methods, including polymer infiltration and pyrolysis (PIP)[6-7], chemical vapor infiltration (CVI)[8] and hot-pressing (HP) [9], *etc*. However, conventional reactive melt infiltration utilizes pure Si as infiltration medium. Limited by its melting point, the infiltration temperature is high and usually around 1450 ℃, which is prone to cause damage to fibers and interfaces, resulting in degradation of mechanical properties[10-12].

In order to solve the problem, low temperature melt infiltration techniques were developed by many researchers, using low melting point Si based alloys as infiltration medium instead of pure Si. Aoki *et al*.[13] prepared SiC_f/SiC-$HfSi_2$ composites by melt infiltration of Si-8.5%Hf alloy(in atom) into SiC_f/C preform at a

Received date: 2023-02-22; **Revised date:** 2023-04-20; **Published online:** 2023-05-15
Foundation item: National Natural Science Foundation of China (52172111, 51872310); National Key R&D Program of China (2022YFB3707700)
Biography: SUN Xiaofan (1998–), male, Master candidate. E-mail: 2487801767@qq.com
孙小凡(1998–), 男, 硕士研究生. E-mail: 2487801767@qq.com
Corresponding author: JIN Xihai, professor. E-mail: jinxihai@hotmail.com; DONG Shaoming, professor. E-mail: smdong@mail.sic.ac.cn
靳喜海, 研究员. E-mail: jinxihai@hotmail.com; 董绍明, 研究员. E-mail: smdong@mail.sic.ac.cn

relatively low temperature of 1375 ℃. In comparison with SiC_f/SiC composites prepared by conventional melt infiltration method at 1400 ℃, the fibers and interphases in the composite were much better preserved, leading to a significant improvement in its mechanical property. Bending strength of the SiC_f/SiC-$HfSi_2$ composite reached a high value of 590 MPa, almost 35% higher than that of conventional melt infiltrated SiC_f/SiC. Similar phenomena were also observed in SiC_f/SiC-$TiSi_2$ composite prepared by low temperature melt infiltration using Si-16%Ti alloy(in atom)[14]. The composite obtained through melt infiltration at 1375 ℃ showed an approximately 70% increasement in tensile strength to 290 MPa, because of the little fiber and interphase damage. Except from SiC_f/SiC composites, the technique of low temperature infiltration also showed great benefit for the fabrication of carbon fiber reinforced ceramic matrix composites as well. Recently, C_f/Si-Y-C composite was successfully prepared at a low infiltration temperature of 1280 ℃, using Si-18%Y eutectic alloy(in atom) as infiltration medium, achieving great success for the protection of fibers and interphases[15].

Due to its high thermal conductivity and the second phase dispersion reinforcement effects, the incorporation AlN particles into SiC by forming AlN-SiC multiphase ceramics endows the material with significantly improved thermal and mechanical properties. In addition, according to the previous researches, AlN-SiC multiphase ceramics show more superior oxidization resistance over monolithic SiC[16]. The additive effects of the above phenomena make AlN-SiC multiphase ceramics a promising candidate for the matrix of SiC_f/SiC composite.

In this work, the fabrication of AlN-SiC multiphase ceramics by low temperature melt infiltration was studied, using porous C-Si_3N_4 as infiltration preform and low melting point Si-Al alloy as the infiltration medium. It is hoped that AlN-SiC multiphase ceramics with superior thermal and mechanical properties can be obtained through the chemical reaction between C, Si_3N_4 and Si, Al. This may pave the way for the fabrication of high performance SiC_f/AlN-SiC composite through low temperature melt infiltration.

1 Experimental

1.1 Preparation of porous C-Si_3N_4 infiltration preform

Porous C-Si_3N_4 infiltration preform was prepared by tape-casting, followed with lamination and high temperature pyrolysis. Firstly, commercial available α-Si_3N_4 (particle size of 0.5 μm), carbon black (particle size of 20 nm) and phenolic resin were ball milled for 8 h in ethanol absolute. Castor oil was used as dispersant. Then suitable amounts of Polyvinyl butyral (PVB) and Dibutyl phthalate (DBP) were added as binder and plasticizer. To ensure slurry homogeneity, the slurry was continuously ball milled for another 24 h and casted into tapes of 0.5 μm in thickness on a tape-casting machine.

The green tapes obtained were cut into pieces with size of 60 mm × 60 mm and warm laminated at 140 ℃ and 1.5 MPa for 40 min in oven to ensure complete curing of the phenolic resin and good adhesion between different layers. Porous C-Si_3N_4 infiltration preforms were obtained after pyrolyzing the laminates at 1200 ℃ for 1 h in argon. According to the difference in carbon content, two types of porous preform were prepared, which were denoted as LCP and HCP preform, respectively. The HCP preform was prepared from C-Si_3N_4 slurry containing more phenolic resin than that used for LCP preform preparation. The composition of the different slurries was given in Table 1.

1.2 Preparation of AlN-SiC multiphase ceramics by low temperature reactive melt infiltration

AlN-SiC multiphase ceramics were prepared by low temperature melt infiltration in vacuum at 1350–1400 ℃ for 40 min, using Si-Al alloy powder or ingot with a nominal mass composition of 70%Si-30% Al as the infiltration medium. The furnace was flushed twice with high purity argon, then vacuum pumped to a gas pressure of ~1 Pa at room temperature before heating. During the whole melt infiltration process, the vacuum level in the furnace was kept to 1–8 Pa. AlN-SiC multiphase ceramic was obtained after the melt infiltration process finished, which was taken out from furnace and double-side machined to a thickness of 4 mm. Hereby residual Si-Al alloy on the surface could be completely removed.

1.3 Tests and characterization

The porosity and pore size distribution of the C-Si_3N_4 porous infiltration preforms were characterized by mercury porosimetry method (AutoPoreIV 9510, Micromeritics,

Table 1 Chemical composition of the slurries used for different types of C-Si_3N_4 infiltration preform preparation

Material	Mass percent of LCP/%	Mass percent of HCP/%
α-Si_3N_4	20.17	15.66
Carbon black	8.65	6.71
Phenolic resin	17.29	26.85
Dibutyl phthalate (DBP)	5.76	4.47
Polyvinyl butyral (PVB)	7.20	5.59
Castor oil	0.58	0.45
Ethanol absolute	40.35	40.27

Shanghai, China). The oxygen content of the Si-Al alloy was determined with a nitrogen-oxygen analyzer (LECO, USA, model TC600C). Phase compositions of AlN-SiC multiphase ceramics were characterized by XRD (D8 ADVANCE, Bruker AXS, Germany). The microstructure of the C-Si_3N_4 infiltration preform and AlN-SiC multiphase ceramics were characterized by field emission scanning electron microscope (FESEM) (Magellan 400, FEI company, USA). Elemental analysis was performed on an energy dispersive spectrometer (EDS, Aztec X-Max 20, Oxford, UK).

The density of the AlN-SiC ceramic was tested by Archimedes' method with deionized water as the immersing medium. Its hardness was tested on a Vickers hardness tester (TUKON-2100B, USA) under an indenter load of 29.4 N and dwelling time of 15 s. The flexure strength was evaluated on a 3-point bending test machine (DDL20, Changchun Research Institute for Mechanical Science Co. Ltd, Changchun, China) at a cross-head speed of 0.5 mm/min and span of 30 mm, using specimens with the size of 3 mm × 4 mm × 50 mm. The specific heat, thermal diffusivity and thermal conductivity were measured on a laser flash thermal conductivity meter (NETZSCH LFA467 HT, Germany), using specimens of ϕ10 mm×2.2 mm in dimension.

2　Results and analysis

Fig. 1 shows the SEM images of the LCP and HCP preforms. The LCP preform shows a homogeneous microstructure with tiny pores uniformly distributed in the C-Si_3N_4 matrix (Fig. 1(a)). High magnification SEM observation reveals that it is composed of well distinguishable C and Si_3N_4 particles, which are loosely packed, forming interconnecting networks. In contrast, a great difference in microstructure is observed for the HCP preform. Due to its high content of phenolic resin derived carbon, the HCP preform shows a typical dual phase microstructure, with large C-Si_3N_4 islands separated by fissure-like pores (Fig.1 (c)). In the C-Si_3N_4 islands, carbon black and Si_3N_4 particles are bonded together by phenolic resin derived carbon, leading to the formation of relatively dense C-Si_3N_4 aggregates. Therein, C and Si_3N_4 particles can hardly be distinguished from each other (Fig. 1(d)).

Fig. 2 shows the mercury porosimetry results of the LCP and HCP preforms. Although both samples show a single modal pore size distribution, their pore size distribution ranges are rather different. Pores in the LCP preform are mainly distributed in a diameter range of 0.06–0.4 μm, while those in the HCP preform are mainly distributed in a diameter range of 0.11–1.1 μm. The pore size distribution range of the HCP preform is nearly three times broader than that of the LCP. Moreover, in comparison with the LCP preform, the average pore size of HCP preform is also much larger. According to the peak position of the pore size distribution curve in Fig. 2(b), the average pore size of the HCP preform is about 0.33 μm, which is almost doubled over that of the LCP preform (0.17 μm). The mercury porosimetry results are in good agreement with the microstructure observation in Fig. 1.

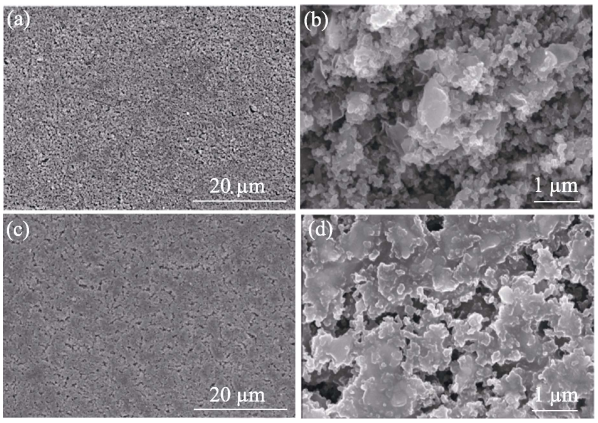

Fig. 1　SEM images of porous C-Si_3N_4 infiltration preforms with different carbon contents
(a, b) Low carbon content preform (LCP); (c, d) High carbon content preform (HCP)

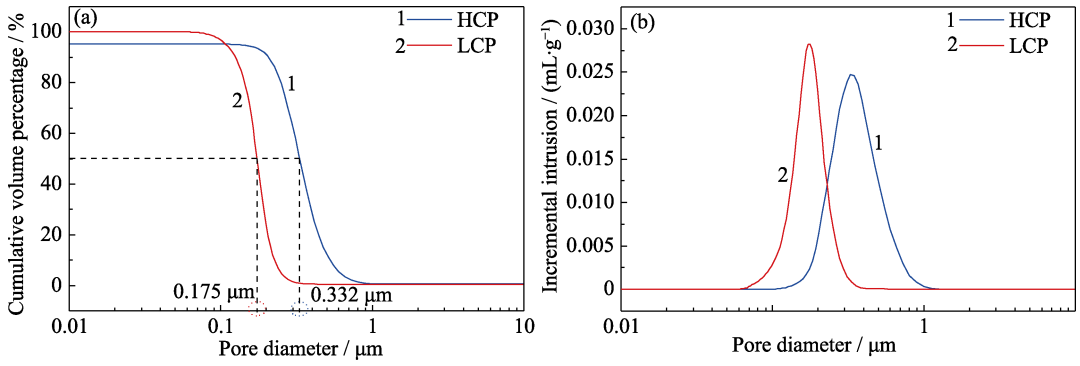

Fig. 2　Mercury porosimetry curves of the C-Si_3N_4 infiltration preforms with different carbon contents
(a) Cumulative volume percentage *vs* pore diameter; (b) Incremental intrusion *vs* pore diameter

Using Si-Al alloy powder (average particle size of 48.5 μm) and ingot as infiltration media, the effects of Si-Al source on its infiltration behavior into the C-Si_3N_4 preform is studied, as shown in Fig. 3. It is found that when Si-Al ingot is used as the infiltration medium, a through-thickness penetration of Si-Al melt into the C-Si_3N_4 preform occurs, resulting in the formation of dense AlN-SiC multiphase ceramics, as revealed below. No special feature except some isolated large SiC particles are observed near the melt-ceramics interface. However, when Si-Al powder is used as the infiltration medium, the things are quite different. A dense interface layer with thickness of 7–15 μm is formed between the Si-Al melt and the C-Si_3N_4 preform, which hinders the penetration of Si-Al melt into the latter. In consequence, the C-Si_3N_4 preform still remains porous after the melt-infiltration process. EDS line scanning finds that this interface layer is mainly composed of Al and O. The formation mechanism of this Al–O interface layer is not clear which could probably be understood as follows.

Due to the strong affinity of Al and Si with O, surface oxidation of Si-Al alloy is inevitable when it is exposed to ambient atmosphere. Especially for the Si-Al alloy powder, surface oxidation is more serious, because of its large surface area. This is testified by the high oxygen mass content of Si-Al alloy powder (0.9%) in comparison with Si-Al ingot (0.18%). The oxygen exists in the form of Al_2O_3 and SiO_2. Under the assistance of high vacuum during melt-infiltration process, the following reactions might occur even before the complete melting of alloy powder:

$$4Al + SiO_2 \rightarrow Si + 2Al_2O\uparrow \quad (1)$$

$$4Al + Al_2O_3 \rightarrow 3Al_2O\uparrow \quad (2)$$

Hereby, the formation of the Al–O interface layer could probably be a result of the surface deposition of the Al_2O species on the C-Si_3N_4 preform.

Furthermore, aside from the surface oxidation of Si-Al powder, another source of oxygen couldn't be neglected. According to thermodynamic calculation, the critical partial pressure of oxygen for Al oxidation is 4.260×10^{-39}–4.257×10^{-27} Pa at 1073–1373 K[17]. While under the experimental conditions in the present work, the oxygen partial pressure in the furnace is probably much higher than the above critical values even though the furnace is flushed twice with high purity argon before heating. The *in-situ* surface oxidation of Si-Al alloy powder might be another source of oxygen for the formation of the Al–O interface layer.

With Si-Al ingot as the infiltration medium, AlN-SiC multiphase ceramics are prepared through reactive melt infiltration of the LCP and HCP preforms, according to reactions:

$$4Al(l) + Si_3N_4(s) \rightarrow 4AlN(s) + 3Si(s) \quad (3)$$

$$Si(l) + C(s) \rightarrow SiC(s) \quad (4)$$

Fig. 4(a) shows XRD patterns of the materials obtained. Independent of the types of C-Si_3N_4 preforms used, both materials show distinctive diffraction peaks of SiC and AlN, no impurity phases other than residual Si

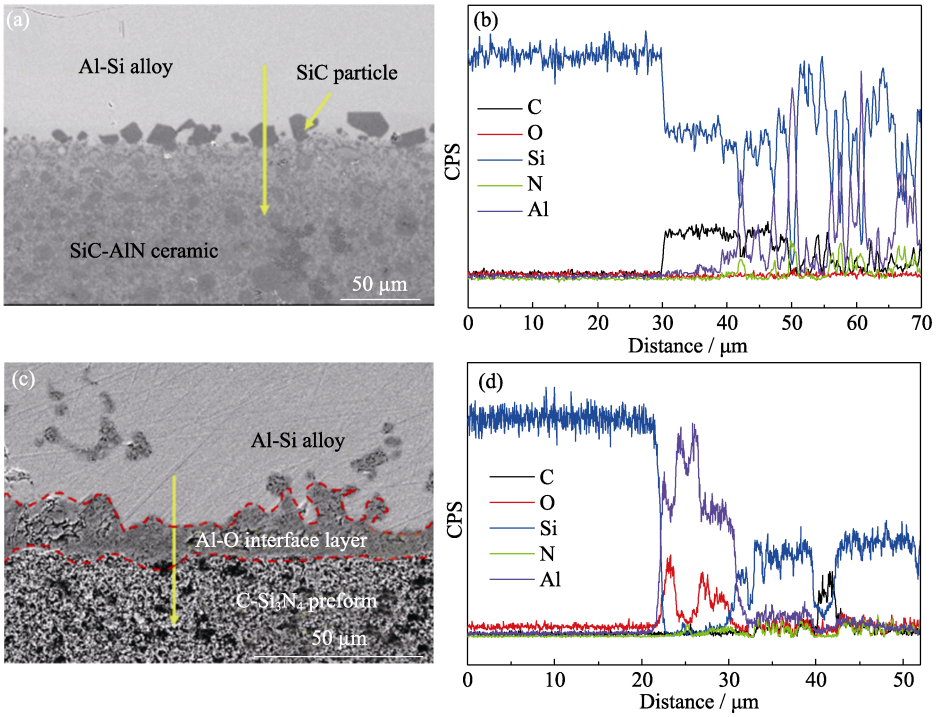

Fig. 3 SEM image and EDS line scanning of the melt/preform interface region in the post melt infiltrated Si-Al/C-Si_3N_4 system, using (a, b) Si-Al ingot and (c, d) Si-Al powder as infiltration medium

Colorful figures are available on the website

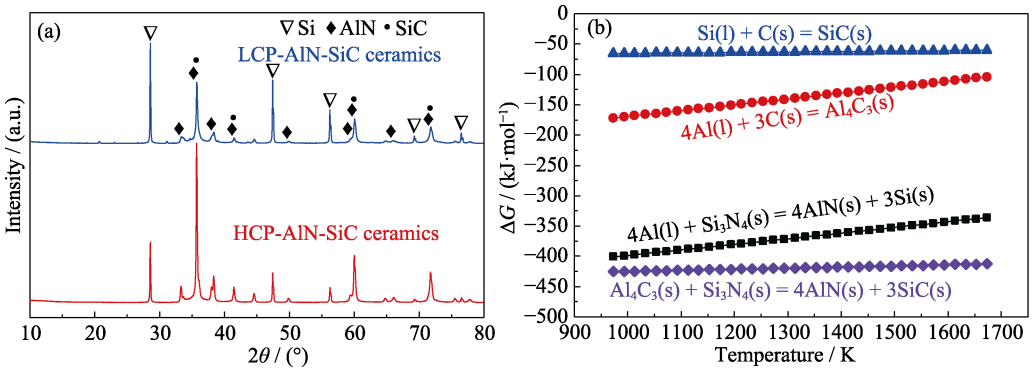

Fig. 4　(a) XRD patterns of AlN-SiC multiphase ceramics prepared from different types of C-Si_3N_4 preform, and (b) changes of standard Gibbs free energy of reaction (3–6) as a function of temperatures calculated with HSC 6.0 software

are detected, especially Al_4C_3. This is to some extent out of expectation, if the coexistence of Al and C in the reaction system is considered, which makes the formation of Al_4C_3 highly possible:

$$4Al(l) + 3C(s) \rightarrow Al_4C_3(s) \quad (5)$$

To understand the above phenomenon, the standard Gibbs free energy changes of reaction (3–5) are calculated together with that of reaction (6):

$$Al_4C_3(s) + Si_3N_4(s) \rightarrow 4AlN(s) + 3SiC(s) \quad (6)$$

It is found that all these reactions show a negative free energy change (Fig. 4(b)). In other words, all above reactions might occur during the reactive melt infiltration process. However, compared with reaction (5), the free energy change of reaction (4) and (6) are more negative. This means that in comparison with Al_4C_3 formation, the formation of AlN in the reaction system is thermodynamically more favorable. For thermokinetics reason, even if Al_4C_3 intermediate phase could be formed during the melt infiltration process, it would convert to AlN by further reaction with Si_3N_4. Hereby, on the basis of thermodynamic calculation results, the absence of Al_4C_3 impurity phase in the final melt infiltrated products is quite reasonable.

Fig. 5 shows SEM and element mapping images of the AlN-SiC multiphase ceramics prepared from different C-Si_3N_4 preforms. As can be seen that both materials show highly dense microstructures without obvious pores. Element mapping indicates a homogeneous distribution of AlN and SiC, although they are almost indiscernible under SEM observation, because of the very close average atomic numbers of them. Residual Si, which is white in color in the SEM images, its content is much higher for the material prepared from the LCP preform. This is in consistent with the strong diffraction peaks of Si in its XRD pattern. Semi-quantitative XRD analysis indicates that residual Si content of the material prepared from LCP preform is about 13%, almost two times higher than that of the material prepared from the HCP preform (4%, in mass). The difference in residual Si content significantly affects the mechanical properties of the AlN-SiC ceramics.

The AlN-SiC ceramics prepared from LCP preform show relatively low strength and hardness of 198.3 MPa and 12.8 GPa, because of its high content of residual Si, which is mechanically weak in comparison with SiC and AlN. In contrast, for the AlN-SiC ceramics prepared from HCP preform, a remarkable improvement in its mechanical properties is observed, due to the significant reduction in its residual Si content. The strength and hardness of this material reached 320.1 MPa and 16.9 GPa, comparable to those of the conventional reaction bonded SiC(Table 2).

Fig. 6 (a, b) show the thermal diffusivities and specific heats of the above AlN-SiC ceramics. Both materials

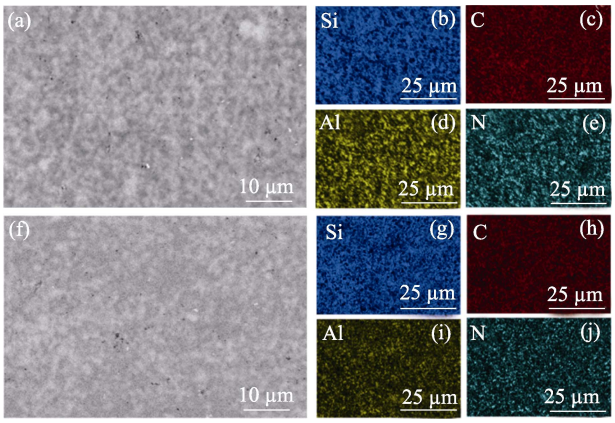

Fig. 5　SEM images of AlN-SiC multiphase ceramics prepared from different C-Si_3N_4 preforms and their corresponding EDS mapping

(a-e) Low carbon content preform; (f-j) High carbon content preform

Table 2　Density and mechanical properties of AlN-SiC multiphase ceramics prepared from different types of C-Si_3N_4 preform

Preform type	Bulk density/ ($g \cdot cm^{-3}$)	Hardness/GPa	Bending strength/MPa
LCP	2.83	12.8±0.2	198.3±4.6
HCP	2.95	16.9±0.4	320.1±25.1

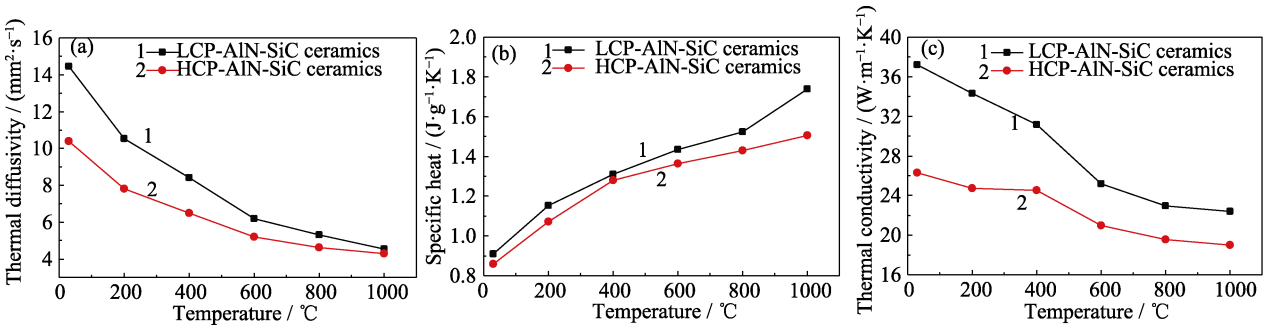

Fig. 6 Thermal diffusivity (a), specific heat (b) and thermal conductivity (c) of AlN-SiC ceramics prepared from the LCP and HCP preforms

demonstrate a significant decrease in their thermal diffusivities as the temperature increases, due to the intensified phonon scattering. While their specific heats increase steadily with increasing temperature, which is in good agreement with the Debye theory prediction.

Based on the thermal diffusivity and specific heat measurements, thermal conductivities of these materials are calculated, according to equation (7):

$$\lambda = \alpha \cdot C_p \cdot \rho \quad (7)$$

where α, C_p and ρ represent the thermal diffusivity, specific heat and bulk density of the materials, respectively. Just like the thermal diffusivities, the thermal conductivities of these materials decline continuously with increasing temperature (Fig. 6(c)). Taking the AlN-SiC ceramics prepared from LCP preform as an example, it shows a thermal conductivity of 37.2 $W \cdot m^{-1} \cdot K^{-1}$ at room temperature. When the temperature increases to 1000 ℃, a great drop in its thermal conductivity to 22.4 $W \cdot m^{-1} \cdot K^{-1}$ is observed. Similar phenomenon is also observed for the AlN-SiC ceramics prepared from HCP preform, although the magnitude of their thermal conductivities is rather different.

In comparison with its counterpart prepared from the HCP preform, the thermal conductivity of the AlN-SiC ceramics prepared from the LCP preform is generally much higher, especially at low temperature. Although the thermal conductivity difference between them gets gradually narrower at high temperature, it still reaches 3.4 $W \cdot m^{-1} \cdot K^{-1}$ at 1000 ℃. As found above, the AlN-SiC ceramics prepared from the LCP contain more residual Si in it, hereby thermal transport contribution from residual Si is one of the possible reasons accounting for the above phenomenon. However, regarding the poor thermal conductivity of Si in comparison with SiC and AlN, this possibility could be excluded. Other possible reasons should be considered.

It is well recognized that grain boundary phonon scattering is one of the main factors affecting the thermal conductivity of ceramic material. The AlN-SiC ceramics prepared from LCP preform contain more residual Si, which presents as liquid phase during the final stage of melt infiltration process. This provides more "free space" for the Oswald ripening grain growth of SiC and AlN particles and leads to the formation of AlN-SiC ceramics with a relatively large grain size and reduces grain boundary phonon scattering. Hereby, a significant improvement in its thermal conductivity could be expected. With respect to the AlN-SiC ceramics prepared from HCP preform, the situations are quite opposite and its thermal conductivity should be comparatively lower. Grain size estimation using the Scherrer equation finds that the average grain sizes of the AlN-SiC ceramics prepared from LCP and HCP preforms are 96.5 and 65.5 nm, respectively, in good agreement with the above hypothesis.

3 Conclusion

AlN-SiC multiphase ceramics were successfully prepared by low temperature reactive melt infiltration (RMI) at 1350 ℃, using Si-Al alloy and porous C-Si_3N_4 as the infiltration medium and preform, respectively. The difference in Si-Al alloy source showed a strong influence on the melt infiltration process. It was more advantageous to use Si-Al ingot as the infiltration medium in comparison with Si-Al powder. When Si-Al ingot was used as the infiltration medium, Si-Al melt could easily infiltrate into the C-Si_3N_4 preform. Under such a circumstance, dense AlN-SiC ceramics with a homogeneous phase distribution could be *in-situ* formed. XRD characterization indicated that it was mainly composed of SiC and AlN, along with different amounts of residual Si, the presence of which significantly affected the properties of the material. The strength and hardness were greatly improved with a decrease in the residual Si content, meanwhile a degradation in the thermal conductivity occurred. The underlying reasons for the above phenomena could find their origins in the poor mechanical properties of Si in comparison with AlN and SiC, as well as the increased grain boundary phonon scattering in the material.

References:

[1] SHEN X, LI M, DAI Y, *et al.* The effects of preparation temperature on the SiC_f/SiC 3D4d woven composite. *Ceramics International*, 2020, **46(9):** 13088.

[2] LIU Y, CHAI N, QIN H, *et al.* Tensile fracture behavior and strength distribution of SiC_f/SiC composites with different SiBN interface thicknesses. *Ceramics International*, 2015, **41(1):** 1609.

[3] YANG B, ZHOU X, CHAI Y. Mechanical properties of SiC_f/SiC composites with PyC and the BN interface. *Ceramics International*, 2015, **41(5):** 7185.

[4] ZHONG Q, ZHANG X, DONG S, *et al.* Reactive melt infiltrated C_f/SiC composites with robust matrix derived from novel engineered pyrolytic carbon structure. *Ceramics International*, 2017, **43(7):** 5832.

[5] CHEN B W, NI D W, WANG J X, *et al.* Ablation behavior of C_f/ZrC-SiC-based composites fabricated by an improved reactive melt infiltration. *Journal of the European Ceramic Society*, 2019, **39(15):** 4617.

[6] MU Y, ZHOU W, WANG H, *et al.* Mechanical and dielectric properties of 2.5D SiC_f/SiC-Al_2O_3 composites prepared *via* precursor infiltration and pyrolysis. *Materials Science and Engineering: A*, 2014, **596:** 64.

[7] SUN X, LIU H, LI J, *et al.* Effects of CVD SiBCN interphases on mechanical and dielectric properties of SiC_f/SiC composites fabricated *via* a PIP process. *Ceramics International*, 2016, **42(1):** 82.

[8] WU P, LIU Y, XU S, *et al.* Mechanical properties and strengthening mechanism of SiC_f/SiC mini-composites modified by SiC nanowires. *Ceramics International*, 2021, **47(2):** 1819.

[9] SANTORO U, NOVITSKAYA E, KARANDIKAR K, *et al.* Phase stability of SiC/SiC fiber reinforced composites: the effect of processing on the formation of α and β phases. *Materials Letters*, 2019, **241:** 123.

[10] CHEN X, FENG Q, GAO L, *et al.* Interphase degradation of three-dimensional C_f/SiC-ZrC-ZrB_2 composites fabricated *via* reactive melt infiltration. *Journal of the American Ceramic Society*, 2017, **100(10):** 4816.

[11] CAO X, YIN X, MA X, *et al.* The microstructure and properties of SiC/SiC-based composites fabricated by low-temperature melt infiltration of Al-Si alloy. *Ceramics International*, 2016, **42(8):** 10144.

[12] TAO P, WANG Y. Improved thermal conductivity of silicon carbide fibers-reinforced silicon carbide matrix composites by chemical vapor infiltration method. *Ceramics International*, 2019, **45(2):** 2207.

[13] AOKI T, OGASAWARA T, OKUBO Y, *et al.* Fabrication and properties of Si-Hf alloy melt-infiltrated Tyranno ZMI fiber/SiC-based matrix composites. *Composites Part A: Applied Science and Manufacturing*, 2014, **66:** 155.

[14] AOKI T, OGASAWARA T. Tyranno ZMI fiber/$TiSi_2$-Si matrix composites for high-temperature structural applications. *Composites Part A: Applied Science and Manufacturing*, 2015, **76:** 102.

[15] GAO Y, LIU Y, WANG J, *et al.* Formation mechanism of Si-Y-C ceramic matrix by reactive melt infiltration using Si-Y alloy and properties of C/Si-Y-C composites. *Ceramics International*, 2020, **46(11):** 18976.

[16] LI Z, GUO R, LI L, *et al.* Improvement in high-temperature oxidation resistance of SiC nanocrystalline ceramics by doping AlN. *Ceramics International*, 2021, **47(21):** 30999.

[17] FUJII H, NAKAE H, OKADA K. Interfacial reaction wetting in the boron nitride/molten aluminum system. *Acta Metallurgica et Materialia*, 1993, **41(10):** 2963.

低温反应熔渗工艺制备 AlN-SiC 复相陶瓷及其性能研究

孙小凡[1,2], 陈小武[1,2], 靳喜海[1,2], 阚艳梅[1,2], 胡建宝[1,2], 董绍明[1,2]

(1. 中国科学院 上海硅酸盐研究所, 高性能陶瓷和超微结构国家重点实验室, 上海　200050; 2. 中国科学院大学 材料与光电研究中心, 北京　100049)

摘　要: AlN-SiC 复相陶瓷力学性能好、导热性与抗高温氧化性能优异, 作为纤维增强陶瓷基复合材料的基体材料具有良好的应用前景。本研究以 Si-Al 合金为熔渗介质, 多孔 C-Si_3N_4 为熔渗预制体, 对低温反应熔渗制备 AlN-SiC 复相陶瓷及其性能展开研究。研究发现 Si-Al 合金形态对反应熔渗过程存在着重要的影响: 以 Si-Al 合金粉末作为熔渗介质时, 反应熔渗过程中在 Si-Al/C-Si_3N_4 界面处将原位形成一层致密的 Al–O 阻挡层, 从而严重阻碍 Si-Al 熔体向 C-Si_3N_4 预制体内部的渗透, 使反应熔渗过程难以进行; 以 Si-Al 合金锭作为熔渗介质时, Si-Al 熔体可以深入渗透到多孔 C-Si_3N_4 预制体内部, 并通过进一步反应, 原位形成致密的 AlN-SiC 复相陶瓷。材料性能测试表明, 所得材料的力学和热学性能与其内部残余硅含量关系密切。随着残余硅含量降低, 材料强度明显提升, 而热导率有所下降。含质量分数 4%残余硅的 AlN-SiC 复相陶瓷, 抗弯强度达到 320.1 MPa, 热导率达 26.3 $W \cdot m^{-1} \cdot K^{-1}$, 材料的强度几乎与传统反应烧结 SiC 陶瓷相当, 并深入探讨了出现上述现象的本质原因。本研究对低温熔渗工艺制备 SiC_f/AlN-SiC 复合材料具有重要的指导意义。

关　键　词: 反应熔渗(RMI); AlN-SiC; 机械性能; 热导率

中图分类号: TB484　　**文献标志码:** A